American Mineralogist, Volume 59, pages 110–119, 1974

The System MgO–Al_2O_3–SiO_2: Solubility of Al_2O_3 in Enstatite for Spinel and Garnet Peridotite Compositions

IAN D. MACGREGOR

University of California, Davis, California 95616

Abstract

The reaction defining the boundary between spinel and garnet peridotite may be used to divide ultramafic rocks into low and high pressure assemblages, respectively. Within each stability field, the Al_2O_3 content of orthopyroxene coexisting with an aluminous phase further divides the conditions of formation within narrower limits. Experimental data in the three-component system MgO–Al_2O_3–SiO_2 illustrate the general nature of the reactions, describe a petrogenetic grid, and provide an approximate assignment for the conditions of formation for Ca-poor ultramafic rocks.

When applied to suites of ultramafic rocks, the data suggest that ultramafic xenoliths and the host mafic lavas are accidentally related. Spinel peridotite xenoliths from alkali basalts are derived from shallower depths with higher geothermal gradients than samples from kimberlite pipes. The rocks from single Alpine peridotites show a wide range of equilibration temperatures and pressures, supporting the hypothesis of their origin as intrusions of mantle material.

Introduction

Three of the major reactions which govern the subsolidus phase chemistry of ultramafic rocks are those which control the boundary between spinel and garnet bearing peridotites ⟨1⟩, and those which control the composition of the pyroxene in equilibrium with olivine and an aluminous phase ⟨2a, 2b⟩. The reactions may be illustrated as follows:

$$Mg_3Al_2Si_3O_{12} + (1-x)Mg_2SiO_4 \rightleftarrows (4-x)MgSiO_3 \cdot xAl_2O_3 + (1-x)MgAl_2O_4 \quad \langle 1 \rangle$$

$$xMgAl_2O_4 + (1+x)MgSiO_3 \rightleftarrows MgSiO_3 \cdot xAl_2O_3 + xMg_2SiO_4 \quad \langle 2a \rangle$$

and

$$xMg_3Al_2Si_3O_{12} + 3(1-x)MgSiO_3 \rightleftarrows 3MgSiO_3 \cdot xAl_2O_3 \quad \langle 2b \rangle$$

If the dependent variables of the reactions may be defined, they may be used to obtain information on the conditions of formation of ultramafic rocks or, along with other geochemical and geophysical data, may be used to help understand the petrological structure of the upper mantle. From univariant reaction ⟨1⟩ we can divide ultramafic rocks into two temperature and pressure fields, while the divariant reactions ⟨2a⟩ and ⟨2b⟩ allow interpretation of the conditions of genesis within the spinel and garnet peridotite stability fields, respectively.

The ternary system, MgO–Al_2O_3–SiO_2, may be used to illustrate the nature of the reactions and to serve as a first approximation of the conditions of formation of ultramafic rocks. Figure 1 illustrates the phase chemistry of a simplified ultramafic rock, and Table 1 gives the composition used in the experiments. Experimentally, we need to define (1) the temperatures and pressures at which spinel peridotite converts to garnet peridotite, and (2) the Al_2O_3 content of pyroxenes in equilibrium with olivine and garnet or spinel.

The reaction defining the boundary between the spinel and garnet peridotites has been previously defined for the ternary system MgO–Al_2O_3–SiO_2 (MacGregor, 1964), the quaternary system CaO–MgO–Al_2O_3–SiO_2 (MacGregor, 1965a; Kushiro and Yoder, 1966; O'Hara, Richardson, and Wilson, 1971), and for multicomponent systems (Green and Ringwood, 1967 and 1970; MacGregor, 1970). The dependence of the reaction on temperature, pressure, and the main compositional variables expected in ultramafic rocks is now fairly well known, and this paper documents the evidence for the simple ternary system. The petrologic, tectonic, and geophysical implications have been previously referred to (Ringwood, MacGregor, and Boyd, 1964; O'Hara, 1967a,b; MacGregor, 1967; Green and Ringwood, 1967 and 1970).

The solid solution of Al_2O_3 in garnet peridotites

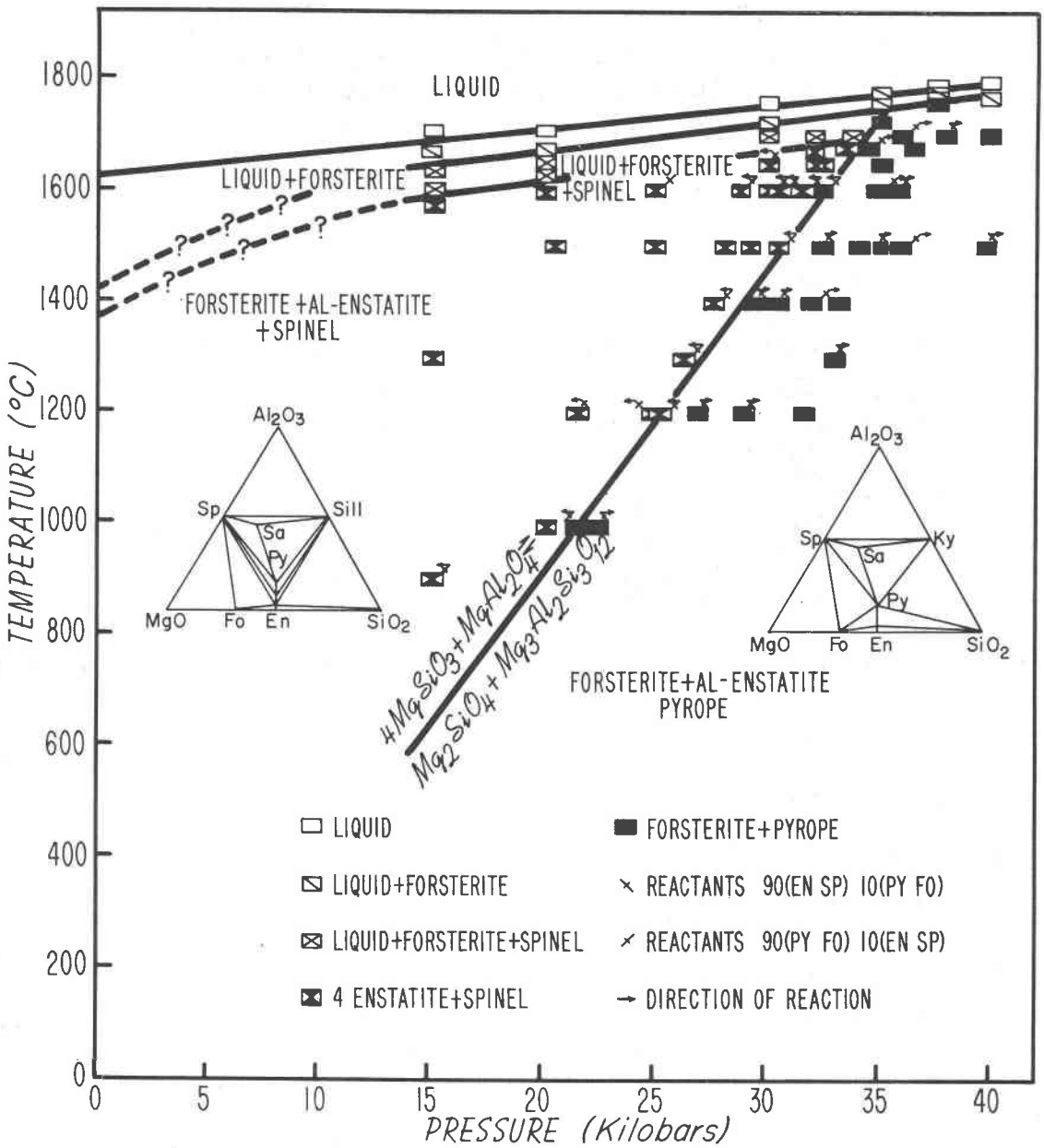

FIG. 1. Experimental determination of the phase chemistry for the composition 4 $MgSiO_3$ + 1 $MgAl_2O_4$ (Table 1).

has previously been examined in the ternary system MgO–Al_2O_3–SiO_2 (Boyd and England, 1964); the quaternary system CaO–MgO–Al_2O_3–SiO_2 (O'Hara, 1963; Boyd, 1969 and 1970); and in multicomponent systems (MacGregor and Ringwood, 1964; Green and Ringwood, 1967). In the spinel peridotite stability field only the CaO–MgO–Al_2O_3–SiO_2 system has been examined (MacGregor, 1965b). A theoretical approach (O'Hara, 1967a,b), using sparse data, has also been used to outline the Al_2O_3 solubility in the plagioclase, spinel, and garnet peridotite stability fields. This paper includes a more detailed analysis of the Al_2O_3 content of orthopyroxenes in the pressure and temperature range from 5 to 40 kilobars and from 900° to 1600°C.

Experimental Results

Reaction ⟨1⟩

The critical results for the reaction $Mg_3Al_2Si_3O_{12} + (1-x)Mg_2SiO_4 \rightleftharpoons (4-x)MgSiO_3 \cdot xAl_2O_3 + (1-x)MgAl_2O_4$ are included in Table 2. Problems

TABLE 1. Composition of Starting Materials.

Composition	Weight per cent MgO	Al_2O_3	SiO_2
4 En + 1 Sp	37.06	18.75	44.29
EnAl - 5	38.16	5.00	56.84
EnAl - 10	36.14	10.00	53.86
EnAl - 15	34.18	15.00	50.82
(EnAl - 7 1/2) + (EnAl - 10)	36.60	8.75	54.65
Pyrope	30.007	25.293	44.697

were encountered in defining the reaction boundary whenever the starting materials were either pure low- or high-pressure crystalline products or glass. The enstatite + spinel reactants could be converted to pyrope + forsterite only at pressure up to 6 kbar in excess of the equilibrium pressure. Correspondingly, when using pyrope + forsterite as the reactants, pressures up to 2 kbar less than the equilibrium pressure were required for detectable reaction. The sluggishness was interpreted as the failure of pyrope and enstatite to nucleate within certain limits of the boundary curve. Thus both starting materials were seeded with 10 wt percent of the products, and a more reliable result, falling between the above two extremes, was obtained. In runs close to the equilibrium curve, reaction rates were slow; at temperatures below 1300°C, little or no reaction took place in experiments up to 48 hours in duration. The addition of water to runs below 1300°C considerably increased reaction rates and allowed the study to be extended down to 900°C. X-ray and microscopic examination did not reveal the presence of amphibole in the products of water-saturated runs.

The solidus and liquidus relationships were outlined using crystalline enstatite + spinel and pyrope + forsterite in their respective stability fields.

The experimentally determined equilibrium boundaries for subsolidus, solidus, and liquidus reactions are given in Figure 1. Equations for the different reactions are as follows:

$$Mg_3Al_2Si_3O_{12} + (1 - x)Mg_2SiO_4 \rightleftarrows (4 - x)MgSiO_3 \cdot xAl_2O_3 + (1 - x)MgAl_2O_4 \quad \langle 1 \rangle$$

$$T = 0.0546P - 173,$$

$$MgSiO_3 + MgAl_2O_4 \rightleftarrows \text{Liquid} + Mg_2SiO_4 + MgAl_2O_4. \quad \langle 2 \rangle$$

$$T = 0.00569P + 1497,$$

$$\text{Liquid} + Mg_2SiO_4 + MgAl_2O_4 \rightleftarrows \text{Liquid} + Mg_2SiO_4. \quad \langle 3 \rangle$$

$$T = 0.00533P + 1560, \quad \text{and}$$

$$\text{Liquid} + Mg_2SiO_4 \rightleftarrows \text{Liquid}. \quad \langle 4 \rangle$$

$$T = 0.00433P + 1620.$$

TABLE 2. Experimental Results Used to Define the Reaction: $(1 - x)Mg_2SiO_4 + Mg_3Al_2Si_3O_{12} \rightleftarrows (4 - x)MgSiO_3 \cdot xAl_2O_3 + (1 - x)MgAl_2O_4$ ⟨1⟩

Temperature (°C)	Pressure (Kilobars)	Reactants	Products	Time
900	15.0	90(Py+Fo) + 10(En+Sp)	En + Sp	30 hrs.
1000	21.1	90(Py+Fo) + 10(En+Sp)	Py+Fo + En+Sp	26 hrs.
1000	22.5	90(En+Sp) + 10(Py+Fo)	En+Sp + Py+Fo	26 hrs.
1200	21.6	90(En+Sp) + 10(Py+Fo)	En + Sp	8 hrs.
1200	24.8	90(Py+Fo) + 10(En+Sp)	En + Sp	7 hrs.
1200	25.0	90(Py+Fo) + 10(En+Sp)	En + Sp	24 hrs.
1200	25.2	90(En+Sp) + 10(Py+Fo)	En + Sp	8 1/2 hrs.
1200	27.0	90(En+Sp) + 10(Py+Fo)	Py + Fo	7 hrs.
1200	29.0	(En + Sp)	Py + Fo	7 1/3 hrs.
1200	30.2	(En + Sp)	Py + Fo	2/3 hrs.
1200	31.7	(En + Sp)	Py + Fo	1 hr.
1300	15.0	90(Py+Fo) + 10(En+Sp)	En + Sp	4 hrs.
1300	26.3	90(Py+Fo) + 10(En+Sp)	En + Sp	7 1/2 hrs.
1300	33.0	(En + Sp)	Py + Fo	6 hrs.
1300	28.1	90(Py+Fo) + 10(En+Sp)	En+Sp + Py+Fo	6 hrs.
1400	27.7	90(Py+Fo) + 10(En+Sp)	En + Sp	5 hrs.
1400	29.5	90(En+Sp) + 10(Py+Fo)	Py + Fo	5 hrs.
1400	30.6	90(En+Sp) + 10(Py+Fo)	En+Sp + Py+Fo	3 hrs.
1400	32.0	[Py + Fo]	Py + Fo	1 1/3 hrs.
1400	33.1	(En + Sp)	Py + Fo	6 1/3 hrs.
1500	20.3	[Py + Fo]	En + Sp	3 hrs.
1500	24.8	[Py + Fo]	En + Sp	1 hr.
1500	27.9	[Py + Fo]	En + Sp	1 1/2 hrs.
1500	29.2	[Py + Fo]	En + Sp	4 hrs.
1500	30.0	[Py + Fo]	Py + Fo	2 hrs.
1500	30.6	90(Py+Fo) + 10(En+Sp)	Py+Fo + En+Sp	1 hr.
1500	32.4	[Py + Fo]	Py + Fo	1 1/3 hrs.
1500	32.7	(En + Sp)	Py + Fo	1 hr.
1500	33.5	(En + Sp)	Py + Fo	1/2 hr.
1500	34.2	(En + Sp)	Py + Fo	2/3 hr.
1500	35.1	(En + Sp)	Py + Fo	2 hrs.
1500	36.0	(Py + Fo)	Py + Fo	4 hrs.
1500	40.1	(En + Sp)	Py + Fo	2 hrs.
1500	45.0	(Py + Fo)	Py + Fo	4 hrs.
1570	15.1	(En + Sp)	En + Sp	5 min.
1600	15.1	(En + Sp)	Q + Fo + Sp	10 min.
1600	20.0	(Py + Fo)	En + Sp	20 min.
1600	28.7	90(En+Sp) + 10(Py+Fo)	En + Sp	1/2 hr.
1600	30.0	(Py + Fo)	En + Sp	20 min.
1600	30.6	90(Py+Fo) + 10(En+Sp)	En + Sp	1/2 hr.
1600	31.5	90(Py+Fo) + 10(En+Sp)	En + Sp	1/2 hr.
1600	32.4	90(En+Sp) + 10(Py+Fo)	En+Sp + Py+Fo	20 min.
1600	34.9	[Py + Fo]	Py + Fo	1/2 hr.
1600	36	(En + Sp)	Py + Fo	1/2 hr.
1630	20	(En + Sp)	Q + Fo + Sp	10 min.
1630	15.1	(En + Sp)	Fo + Sp + ((Q))	10 min.
1650	20.0	90(En+Sp) + 10(Py+Fp)	Q + Fo + Sp	10 min.
1650	30.0	(En + Sp)	En + Sp	10 min.
1650	32.1	(Py + Fo)	En + Sp	15 min.
1650	35.1	[Py + Fo]	Py + Fo	5 min.
1660	14.9	(En + Sp)	Q + Fo	5 min.
1675	32.1	(Py + Fo)	En + Sp	10 min.
1675	20.0	(En + Sp)	Q + Fo	10 min.
1680	33.5	90(Py+Fo) + 10(En+Sp)	Py+Fo + En+Sp	20 min.
1680	34.6	90(Py+Fo) + 10(En+Sp)	Py + Fo	20 min.
1680	36.5	[Py + Fo]	Py + Fo	20 min.
1700	15.1	(En + Sp)	Q	3 min.
1700	30.0	(En + Sp)	Q + Fo + Sp	10 min.
1700	32.1	(Py + Fo)	Q + Fo + Sp	10 min.
1700	32.4	90(Py+Fo) + 10(En+Sp)	Q + Fo + Sp	15 min.
1700	33.8	90(Py+Fo) + 10(En+Sp)	Q + Fo + Sp	15 min.
1700	36.0	90(Py+Fo) + 10(En+Sp)	Py + Fo	20 min.
1700	38.0	(En + Sp)	Py + Fo	15 min.
1710	20.0	(En + Sp)	Q	5 min.
1730	35.1	(En + Sp)	En + Sp	3 min.
1760	30.0	(En + Sp)	Q	3 min.
1760	35.1	(En + Sp)	Q + Fo	3 min.
1760	37.6	(Py + Fo)	Py + Fo	3 min.
1770	40.0	(Py + Fo)	Py + Fo + ((Q))	3 min.
1775	37.6	(En + Sp)	Q + Fo	3 min.
1780	35.1	(En + Sp)	Q + Fo	3 min.
1790	37.6	(En + Sp)	Q	3 min.
1800	40.0	(Py + Fo)	Q	3 min.

( ) = crystalline; [ ] = glass; (( )) = trace; En = Enstatite; Fo = Forsterite; Py = Pyrope; Q = Glass; Sp = Spinel; where products underlined indicates stable phase assemblage; pressure reported as gauge pressure.

Linear extrapolation of the liquidus curve to 1 atmosphere is in agreement with the inferred temperature of Osborn and Muan (1960). However, both solidus curves indicate that below 15 kbar either considerable curvature or inflection of the curves is necessary for agreement between the high pressure and 1 atmosphere data.

As indicated by O'Hara *et al* (1971), the pyroxene entering into the reaction varies in its Al_2O_3 content, and Skinner and Boyd (1964) have shown that the unit cell volume on enstatite decreases with increasing Al_2O_3 solid solution. Thus one may anticipate a change in the ΔV of reaction along the equilibrium boundary, and expect the boundary to be curved rather than linear. O'Hara *et al* (1971) confirm this for the system CaO–MgO–Al_2O_3–SiO_2. In the present study a curvature of the boundary was anticipated, but the data appear to fit best an essentially linear boundary. Apparently the ΔH of reaction is varying in some compensating manner to maintain an essentially uniform slope.

Calculation of the ΔV of reaction is hindered by the lack of information on the thermal expansion and compressibility of all phases, particularly aluminous enstatite, at high temperatures and pressures. However, linear extrapolation of the compressibility and thermal expansion data (Birch, 1966; Skinner, 1966) for the reacting phases, and the assumption that aluminous enstatite is linearly equivalent in its properties to enstatite, leads to the following evaluation (Table 3) of reaction ⟨1⟩ incorporating the effect of Al_2O_3 solid solution in enstatite.

TABLE 3. ΔV of Reaction for $Mg_3Al_2Si_3O_{12} + (1-x)Mg_2SiO_4 \rightleftarrows (4-x)MgSiO_3 \cdot xAl_2O_3 + (1-x)MgAl_2O_4$ ⟨1⟩

Temperature (°C)	Pressure (Kilobars)	Weight per cent Al_2O_3 in Enstatite	ΔV cc/mol	ΔV %
600	13.5	1	-6.361	3.89
856	17.5	3	-5.615	3.46
1026	20.2	5	-4.879	3.03
1205	23	7	-3.864	2.43
1332	25	9	-2.727	1.73
1460	27	11	-1.912	1.23
1571	28.75	13	-0.967	0.63

Reactions ⟨2a⟩ and ⟨2b⟩

The reactions $xMgAl_2O_4 + (1+x)MgSiO_3 \rightleftarrows xMg_2SiO_4 + MgSiO_3 \cdot xAl_2O_3$ and $xMg_3Al_2Si_3O_{12} + 3(1-x)MgSiO_3 \rightleftarrows 3MgSiO_3 \cdot xAl_2O_3$ may be monitored by analyzing the Al_2O_3 content of enstatite in equilibrium with forsterite and garnet or spinel (see Appendix). The Al_2O_3 content of the enstatites is shown in Table 4, and displayed in Figure 2 where Al_2O_3 isopleths have been superimposed to develop a petrogenetic grid. To account for the differences in experimental technique (see Appendix), the reaction boundary between the spinel and garnet peridotites has been plotted using a −10 percent pressure correction. The slopes of the Al_2O_3 solubility curves are inflected at this boundary.

A major limitation to the analyses was the fine grain size of the products an dthe fact that in the spinel stability field the enstatites often occur as poikilitic crystals sieved with spinel. In general, coarser crystals could be obtained in the temperature range from 1100° to 1300°C, but grain size decreased at both higher and lower temperatures. The lack of a balance between the Mg and Si atoms in Table 4 gives some indication of the quality of the analysis and the possible effect of adjacent grains. In those portions of Figure 2 where no data was given, a number of experiments failed to produce samples with a sufficiently coarse grain size. The resultant grain size proved to be a fairly capricious aspect of the experiment, and this problem was not carefully examined. The combination of errors introduced by the temperature, pressure, and analytical uncertainties would suggest that each isopleth has an uncertainty of ±10 percent.

In the garnet stability field, the slope of the Al_2O_3 isopleths is in general agreement to that found by other workers in the three-component system MgO–Al_2O_3–SiO_2 (Boyd and England, 1964), proposed for the four component system CaO–MgO–Al_2O_3–SiO_2 (O'Hara, 1967b), and defined for a multicomponent mantle system (Green and Ringwood, 1967). A single microprobe determination by Boyd (1970) at 1200°C and 30 kbar gives a value of 5.9 wt percent Al_2O_3 for the orthopyroxene coexisting with olivine and garnet. A value of 4.9 was determined for the same point in this study. Since Boyd's experiments were made by advancing the piston (personal communication), one may anticipate a negative correction of about 5 to 10 percent (Johannes *et al*, 1971) to his nominal pressure value. In contrast, the data for this paper were collected by retracting the piston, indicating that the observed pressure is the 'real' pressure to within ±5 percent. A negative correction of 5 to 10 percent applied to Boyd's (1970) data would bring the two values to an equivalence well within the anticipated experimental error.

TABLE 4. Chemistry of Aluminous Enstatites in Equilibrium with Forsterite and Garnet or Spinel Following the Reactions: $xMgAl_2O_4 + (1 + x)MgSiO_3 \rightleftarrows MgSiO_3 \cdot xAl_2O_3 + xMg_2SiO_4$ (2a), and $xMg_3Al_2Si_3O_{12} + 3(1 - x)MgSiO_3 \rightleftarrows 3MgSiO_3 \cdot xAl_2O_3$ (2b).

Starting Composition	Temp. (°C)	Pressure (Kilobars)	Time	Additional Phases	Enstatite Composition (Weight Percent) MgO	Al_2O_3	SiO_2	Total	Enstatite (Atomic Formula [O=3]) Mg	Al	Si
4En + 1Sp	900	5	24 hrs.	Fo + Sp	37.2	7.4	55.4	100.0	.928	.145	.927
4En + 1Sp	900	10	24 hrs.	Fo + Sp	-	5.5	-	-	-	≈.108	-
4En + 1Sp	1000	5	24 hrs.	Fo + Sp	37.6	9.4	53.9	100.9	.932	.550	.897
4En + 1Sp	1000	15	24 hrs.	Fo + Sp	37.0	5.8	55.8	98.6	.935	.116	.945
4En + 1Sp	1000	20	22 hrs.	Fo + Sp	38.3	4.3	57.4	100.0	.960	.084	.960
$EnAl_{10}$ + (Py)	1000	30	63 hrs.	Py	39.0	2.4	58.3	99.7	.979	.048	.977
4En + 1Sp	1100	10	55 1/4 hrs.	Fo + Sp	35.0	9.9	54.3	99.2	.877	.197	.914
4En + 1Sp	1100	15	23 hrs.	Fo + Sp	38.4	7.6	54.9	99.9	.952	.149	.914
4En + 1Sp	1100	20	9 3/4 hrs.	Fo + Sp	-	5.4	56.6	-	-	≈.106	-
$EnAl_{10}$ + (Py)	1100	25	10 1/4 hrs.	Py	37.7	4.7	56.5	98.9	.950	.094	.955
$EnAl_{10}$ + (Py)	1100	30	9 hrs.	Py	37.8	3.3	57.0	98.1	.959	.066	.971
$EnAl_5$ + (Py)	1100	40	75 1/4 hrs.	Py	39.9	1.7	58.0	99.6	1.000	.037	.975
4En + 1Sp	1200	5	24 hrs.	Fo + Sp	-	14.3	-	-	-	≈.280	-
$EnAl_{10}$ + (Py)	1200	25	13 3/4 hrs.	Py	38.9	6.7	55.0	100.6	.967	.132	.918
$EnAl_{10}$ + (Py)	1200	30	13 2/3 hrs.	Py	39.3	4.9	55.5	99.7	.986	.097	.934
$EnAl_{10}$ + (Py)	1200	35	12 3/4 hrs.	Py	38.0	3.1	57.0	98.1	.964	.062	.970
$EnAl_5$ + (Py)	1200	40	75 1/4 hrs.	Py	39.1	2.6	57.6	99.3	.982	.051	.970
4En + 1Sp	1300	10	10 hrs.	Fo + Sp	33.9	15.5	52.0	101.4	.834	.904	.858
4En + 1Sp	1300	15	13 1/2 hrs.	Fo + Sp	36.5	12.4	50.0	98.9	.925	.249	.851
4En + 1Sp	1300	25	6 1/6 hrs.	Fo + Sp	35.2	7.7	54.8	97.7	.895	.156	.935
$EnAl_{10}$ + (Py)	1300	30	6 1/2 hrs.	Py	36.8	6.3	55.0	98.1	.935	.127	.938
50($EnAl_{10}$) + 50($EnAl_{7\ 1/2}$)	1300	30	15 1/2 hrs.	Py	37.8	6.4	-	-	-	≈.135	-
$EnAl_5$ + (Py)	1300	35	15 3/4 hrs.	Py	38.8	4.9	55.4	99.1	.978	.098	.937
$EnAl_{10}$ + (Py)	1300	40	8 1/2 hrs.	Py	39.4	3.2	59.1	101.7	.965	.062	.971
4En + 1Sp	1400	15	3 1/2 hrs.	Fo + Sp	34.9	15.4	51.6	101.9	.855	.298	.849
4En + 1Sp	1400	25	5 1/4 hrs.	Fo + Sp	36.5	10.7	53.7	100.9	.903	.209	.891
4En + 1Sp	1400	30	6 hrs.	Fo + Sp	37.4	8.2	54.8	100.4	.930	.161	.914
$EnAl_{10}$ + (Py)	1400	35	9 hrs.	Py	37.7	6.1	54.3	98.1	.960	.123	.928
4En + 1Sp	1600	25	1/2 hr.	Fo + Sp	-	14.1	36.7	-	-	≈.277	-
4En + 1Sp	1600	30	1/2 hr.	Fo + Sp	36.7	12.0	36.7	101.1	.870	.238	.908

(En = Enstatite; Fo = Forsterite; Py = Pyrope; Sp = Spinel; ( ) = Seed; 4En + 1Sp Composition as Glass).

There are no previous experimental data with which to contrast the Al_2O_3 solid solution of orthopyroxene in the spinel stability field. However, the slope of the Al_2O_3 isopleths is opposite to the negative slopes suggested by theoretical considerations (O'Hara, 1967b), but comparable to the positive slopes for Al_2O_3 solubility in diopside coexisting with forsterite and spinel (MacGregor, 1965b). Anastasiou and Siefert (1972) have examined Al_2O_3 solubility in enstatite coexisting with cordierite plus spinel, and sapphirine plus cordierite up to 5 kbar water pressure. Both assemblages represent phase volumes adjacent to that of the spinel-enstatite-forsterite assemblages, and thus their Al_2O_3 solubility data apply to the present study. At 5 kbar Anastasiou and Siefert's data (1972) indicate that the wt percent Al_2O_3 of an enstatite in equilibrium with a spinel should have maximum values of 4.1, 6.8, and 9.7 at 900°, 1000°, and 1100°C, respectively. The values contrast with values of 7.4, 9.4, and 11.8 (Fig. 2) at 900°, 1000°, and 1100°C found in the present study.

The discrepancy is not understood. The pressure uncertainties at 5 kbar for a solid media device are large, and it is probable that the strength of the materials becomes a proportionately more important contribution to the observed pressure, suggesting that the pressures on the sample may well be significantly lower than recorded. Anastasiou and Siefert (1972) get the same results using X-ray determinative curves and phase-disappearance techniques. Further, their hydrothermal apparatus is better suited to experiments in the 1 to 5 kbar pressure range. Though uncertain, it is probable that their values are correct, and the Al_2O_3 isopleths in Figure 2 should flatten with decreasing pressure much as is observed for diopside in equilibrium with spinel (MacGregor, 1965b).

Application to Geologic Data

Application of the experimental data to define the conditions of formation of natural rocks requires knowledge of the effect of other compositional variables and an independent assignment of either temperature or pressure. Unfortunately, there are no studies available which may adequately be used to fully evaluate the effect of other compositional variables. Boyd (1970) has shown that at 1200°C and

30 kbar the Al_2O_3 content of enstatite in equilibrium with garnet varies from 5.9 to 4 wt percent from the Ca-undersaturated to Ca-saturated assemblage. Thus an enstatite in equilibrium with diopside will have approximately 2 wt percent less Al_2O_3 than an enstatite on the enstatite-pyrope join. Although Figure 2 may be used directly for a Ca-free ultramafic rock such as a harzburgite, adjustments must be made when applied to Ca-saturated, two-pyroxene, ultramafic rocks such as lherzolites. Thus for most ultramafic rocks Figure 2 may only be used in a semiquantitative way; using Figure 2 directly will result in absolute values of pressure that are high, but the relative assignments of pressure for a suite of samples should remain essentially the same. Temperatures may be determined from the mutual solubility of diopside and enstatite (Davis and Boyd, 1966). Although Al_2O_3 solubility affects the diopside-enstatite solvus, Boyd (1970) indicates that this effect is small for low Al_2O_3 contents.

Figure 2 may only be used in cases where both orthopyroxene and clinopyroxene form an equilibrium assemblage with olivine and an aluminous phase

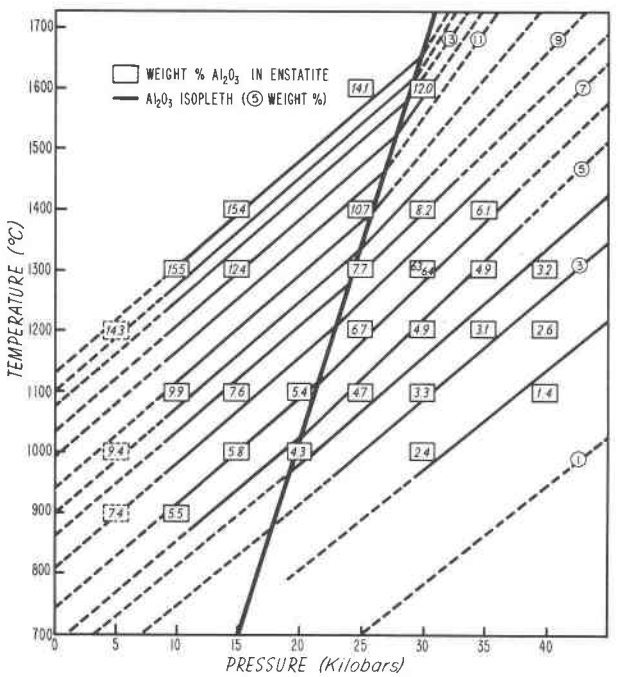

FIG. 2. Al_2O_3 content of enstatite in equilibrium with forsterite and pyrope or spinel (heavy bold line defines reaction boundary for $Mg_3Al_2Si_3O_{12} + (1-x)Mg_2SiO_4 \rightleftarrows (4-x)MgSiO_3 \cdot xAl_2O_3 + (1+x)MgAl_2O_4$; less heavy lines represent Al_2O_3 isopleths whose values (given in circles) represent contents of Al_2O_3 in enstatite ranging from 1 to 15 wt percent.

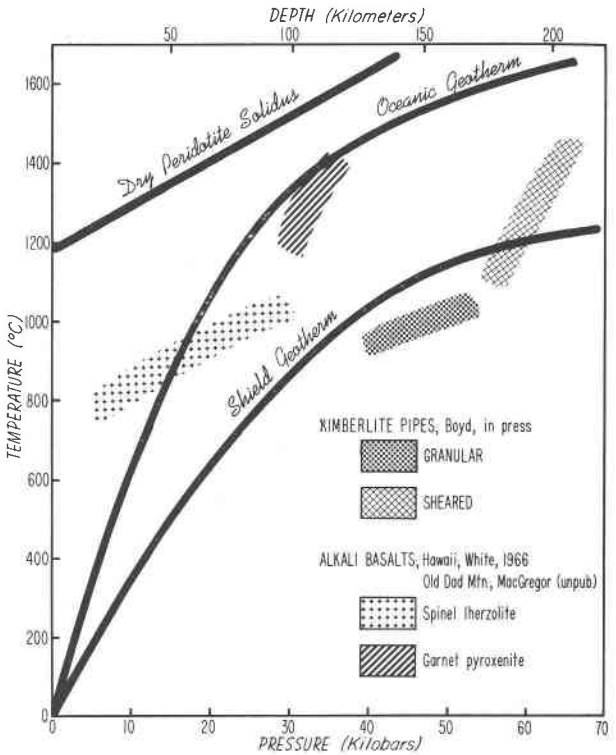

FIG. 3. Interpreted conditions of formation for suites of ultramafic xenoliths from alkali basalts and kimberlites.

(spinel or garnet). Departures from this assumption may be used in the case of garnet or spinel pyroxenites such as those from Hawaii (Beeson and Jackson, 1970) where an olivine-saturated surface is assumed. In cases where the aluminous phase is absent, only a minimum temperature and maximum pressure may be obtained.

Mafic and ultramafic xenoliths included in basalts

Xenoliths from alkali basalts. Spinel peridotite xenoliths from a wide number of localities (Ross, Foster and Myers, 1954; White, 1966; Kutolin and Frolova, 1970; MacGregor, unpublished) exhibit a range of temperatures and pressures which fall within a well defined region of temperature-pressure space (Fig. 3). The wide range of pressures exhiibted by the samples from individual localities indicates that the xenoliths represent accidental fragments of the mantle rather than suites of cognate xenoliths genetically associated with the host magma. Garnet pyroxenites from Hawaii (Beeson and Jackson, 1970) show reconstructed temperatures and pressures in the range 1300 to 1400°C and 30 to 34 kbar (Fig. 3).

Xenoliths from kimberlites. Using the data pre-

sented in this paper, Boyd (in press) has shown that xenoliths from Lesotho kimberlites may be divided into two textural suites (Fig. 3) which correlate with origins from well defined localities in the subcontinental mantle. A suite of granular samples occurs in the temperature range 800 to 900°C and 40 to 50 kbar, whereas sheared xenoliths are characteristically found at temperatures ranging from 1000 to 1400°C and pressures of 45 to 70 kbar. A comparable division has been found by J. Johnston (unpublished) for the Jagersfontein kimberlite pipe. As with the spinel peridotites, the ultramafic xenoliths from kimberlites appear to be accidental in origin. It is difficult to assign a cognate origin to samples derived over such a wide depth range. Their value lies in recording some information on ambient conditions in, and data pertaining to a petrographic profile of, the upper mantle.

Discussion. Boyd (in press) has suggested that the Lesotho samples record a Cretaceous geotherm beneath the African shield. The granular samples fall close to a predicted Shield geotherm (Ringwood *et al,* 1964), while the anomalously high geotherm shown by the sheared samples records the thermal effects of shearing in the Low Velocity Zone during the period of Cretaceous drift. The "knee" shown by the xenoliths represents the top of the Low Velocity Zone.

Although the data is not comparably complete, a similar interpretation may be applied to the xenoliths from Hawaii. The spinel peridotites mark the location of an oceanic geotherm, while the garnet pyroxenites record the thermal transient associated with the current period of drift. The "knee" is again thought of as the top of the oceanic Low Velocity Zone. The garnet pyroxenites are samples from the Low Velocity Zone while the spinel peridotites are derived from the superjacent lithospheric plate.

The discrepancy between the calculated Shield and Oceanic geotherms (Clark and Ringwood, 1964) and the interpretations presented in this paper may be anticipated. The calculated values represent a static mantle model cooling by conduction alone, while the paleogeotherms recorded by the xenoliths probably reflect the variable effects associated with the dynamics of drifting and convective cooling. The effects of other components would suggest that the allocation of temperatures and pressures in Figure 3 are on the high pressure side. It is probable that the predicted geothermal gradients will be slightly steeper and move to lower pressures. However, the relative positions of the samples will remain essentially intact. Data is not currently available to make a quantitative statement of the anticipated errors introduced by other compositional variables.

Alpine peridotites

Data from Alpine peridotites (Green, 1964; MacGregor, 1962; Challis, 1965; Loney, Himmelberg, and Coleman, 1971; Onuki and Tiba, 1965; Medaris, 1972; Himmelberg and Loney, 1973) invariably indicate equilibrium over a wide range of temperatures and pressures. In a number of cases, textural and mineral chemical evidence (Green, 1964; Challis, 1965; Loney *et al,* 1971; Medaris, 1972) indicate more than one generation of samples from a single intrusion. The different textural types indicate equilibria over a wide range of temperatures and pressures, possibly recording the path along which the different intrusions migrated to the surface. It is apparent that the interpretation of any single intrusion is a complex matter, and that suites of samples need study before any interpretation is made. Single samples are meaningless for these dynamic phenomena in which the lack of complete equilibrium for the solid-solid reactions results in a "memory" outlining the path of any single intrusion to the surface.

The sparse data in Figure 4 suggest two main lines of ascent for Alpine peridotites. The Mount Albert and Lizard intrusions appear to be close to an oceanic geotherm; in contrast the circum-Pacific peridotites outline a path suggesting an origin from considerably lower temperatures and higher pressures. At present an interpretation as to the difference is not clear, although one speculation is that the high temperature Mount Albert and Lizard intrusions arise from regions of high geothermal gradients such as spreading centers, while the circum-Pacific examples originate from regions with depressed geothermal gradients such as a subduction zone.

It should be noted that the lower temperatures assigned to the Southwest Oregon peridotites by the diopside-enstatite geothermometer (Davis and Boyd, 1966) contrast with the higher values preferred by Medaris (1972) from Mg/Fe partitioning. The higher temperatures would indicate an association with the high-temperature peridotites rather than the circum-Pacific suite. These problems are not resolved in this paper; however it does seem possible to conclude that the samples from single intrusions show a range of temperatures and pressures of equilibration. Further, the range of values is related to the tectonic

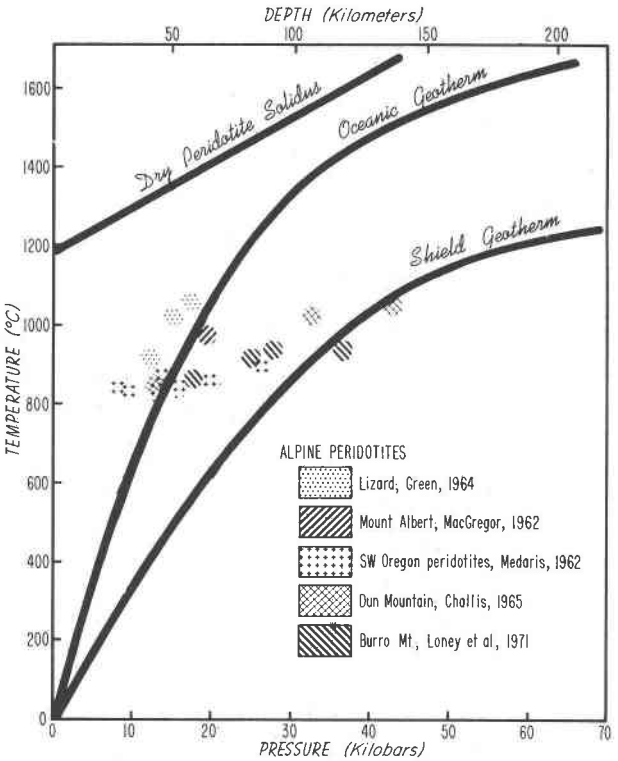

FIG. 4. Interpreted conditions of formation for samples from different Alpine peridotites.

environment of intrusion, which gives useful insight in distinguishing different types of Alpine peridotites.

Metamorphosed ultramafic rocks

Examples of metamorphosed ultramafic rocks are provided by the Norwegian garnet peridotites (O'Hara and Mercy, 1963). These are generally located along the Shield geotherm, suggesting that they have been intruded into their present location.

The wide distribution of temperatures and pressures indicated by all the examples cited above illustrates the need for comprehensive studies on individual localities. Single isolated samples are of little value in illustrating the dynamics of intrusion or the range of conditions along a geothermal gradient, and can seldom be said to be representative.

APPENDIX

Experimental Method

Apparatus

All the experiments were made using a solid media, $\frac{1}{2}$ inch (1.27 cm) diameter piston and cylinder device (Boyd and England, 1960), with a solid-media furnace assembly constructed according to Boyd and England's (1963) design.

Experimental Uncertainties

Pressure. In all the experiments used to define reaction ⟨1⟩, the samples were brought to temperature at the gauge pressure listed in Table 2. Subsequent piston-in adjustments were made to maintain nominal gauge pressure during the course of the experiment. Experiments in furnace assemblies comparable to that used in the present study suggest that the above procedure demands a correction varying from −8 percent to −11 percent of gauge pressure (Johannes *et al,* 1971; Green *et al,* 1966). Gauge or ram pressures are listed in Table 2, and used in Figure 1, but the discussion includes a −10 percent correction to all values, which should give values to within ±3 percent of the true value.

In the experiments used to define the Al_2O_3 solid solution in orthopyroxenes (reactions 2a and 2b), the pressure was first raised to a value 3 kbar above the gauge pressure (listed in Table 3), then the temperature was raised to the desired value, and the piston retracted to give the nominal gauge pressure. Boyd *et al* (1966) suggest that for this procedure the gauge pressure is within 5 percent of the "true" pressure.

Temperature. Temperature uncertainties arise from (1) thermal gradients across the sample, (2) minor fluctuations during the experiment, and (3) a pressure effect on the thermocouple. Measured thermal gradients across the sample varied from less than 10° at 1000°C, to 15°C at 1800°C, while temperature fluctuations during the experiments were held to with ±3°C. Corrections for the pressure effect on the thermocouple *e.m.f.* were not made.

Starting Materials

The starting material used to define reaction 1 was composed of four crystalline assemblages of the same bulk composition (Table 1). These were:

1) 4 enstatite + 1 spinel,
2) forsterite + pyrope,
3) 90% (4 enstatite + spinel) + 10% (forsterite + pyrope), and
4) 90% (forsterite + pyrope) + 10% (4 enstatite + spinel).

For runs used to define the solution of Al_2O_3 in orthopyroxene, the starting composition was dependent on whether the experiment was conducted in the spinel or garnet stability field. For all runs in the

spinel stability field, a glass of the composition 4 enstatite + spinel (Table 1) was used. In the garnet stability field, various glasses along the join enstatite-pyrope, seeded with crystalline pyrope, were used as the starting material (Table 2).

Both graphite and platinum capsules were used. Where duplicate experiments were made, no differences in results were observed. In general, graphite was used for experiments made at temperatures in excess of 1200°C, and platinum capsules for temperatures of 1200°C or less. Experiments made in excess of 1300°C were dried for 45 minutes at 1000° C in a dry nitrogen furnace; those at 1300°C were not dried, and water was added to those at 1200°C and lower temperatures.

Analysis of Products

Crushed powders of the reactants for reaction ⟨1⟩ were examined with petrographic microscope and by X-ray diffraction techniques. For definitive experiments close to the reaction boundary, reaction was considered to have proceeded only if there was significant contrast between the diffractograms of the seeded reactants and products.

The Al_2O_3 content of orthopyroxenes in equilibrium with garnet or spinel was determined with a MAC electron-microprobe. The major limitation of this technique was the grain size of the orthopyroxene grains. In general the grains varied from fractions of a micron to about 10 microns in diameter, although grains as large as 80 microns were found in a few samples. Grains smaller than 5 microns were considered unsuitable. Wherever possible three grains were analyzed from each experiment; the triplicate analyses seldom differed by more than ±10 percent of the mean. A program written by Brown (1965) was used to calculate for absorption and fluorescence corrections; no atomic number corrections were used. The best indication of the quality of the analysis appeared to be the balance of Al^{+++} in the octahedral and tetrahedral sites, rather than their summation to 100 percent. In general there was a balance to within ±5 percent, suggesting the ±5 percent value is a better estimate of analytical error, rather than the ±2 percent expected for a probe analysis. The increased error probably results from the fine grain size, and the probability of interfering effects from adjacent grains.

Acknowledgments

The experimental data used to define reaction ⟨1⟩ were collected while the author was a fellow at the Geophysical Laboratory, Washington. I am indebted to Dr. F. R. Boyd for the use of the high pressure equipment, and for his advice and assistance. The microprobe analyses were similarly conducted at the Geophysical Laboratory; the assistance and the instruction of C. Hadidiakos are gratefully acknowledged.

The experiments used to define Al_2O_3 solubility in the orthopyroxenes were conducted at the Southwest Center for Advanced Studies with support from the United States Army Research Office (Contract: DA-31-214-ARO-D-463).

The paper has benefitted from the advice and criticisms of the reviewers; A. L. Boettcher, F. R. Boyd, G. Medaris, and D. C. Presnall are thanked for this effort.

References

ANASTASIOU, P., AND F. SIEFERT (1972) Solid solubility of Al_2O_3 in enstatite at high temperatures and 1–5 Kb water pressure. *Contrib. Mineral. Petrology,* **34,** 272–287.

BEESON, M. V., AND E. D. JACKSON (1970) Origin of garnet pyroxenite xenoliths at Salt Lake Crater, Oahu. *Mineral. Soc. Amer. Spec. Pap.* **3,** 95–113.

BIRCH, F. (1966) Compressibility; Elastic constants. *In,* S. P. CLARK, Ed., *Handbook of Physical Constants. Geol. Soc. Amer. Mem.* **97,** 97–173.

BOYD, F. R. (1969) The system $CaSiO_3$–$MgSiO_3$–Al_2O_3. *Carnegie Inst. Wash. Yearbook,* **68,** 214–221.

——— (1970) Garnet peridotites and the system $CaSiO_3$–$MgSiO_3$–Al_2O_3. *Mineral. Soc. Amer. Spec. Pap.* **3,** 63–75.

——— (1973) The pyroxene geotherm. *Geochim. Cosmochim. Acta* (in press).

———, AND J. L. ENGLAND (1960) Apparatus for phase-equilibrium measurements at pressures up to 50 kilobars and temperatures up to 1750°C. *J. Geophys. Res.* **65,** 741–748.

———, AND ——— (1963) Effect of pressure on the melting of diopside, $CaMgSi_2O_6$, and albite, $NaAlSi_3O_8$ in the range up to 50 kilobars. *J. Geophys. Res.* **68,** 311–323.

———, AND ——— (1964) The system enstatite-pyrope. *Carnegie Inst. Wash. Yearbook,* **63,** 157–161.

———, P. M. BELL, J. L. ENGLAND, AND M. C. GILBERT (1966) Pressure measurement in a single-stage apparatus. *Carnegie Inst. Wash. Yearbook,* **65,** 410–414.

———, AND I. D. MACGREGOR (1964) Ultramafic rocks. *Carnegie Inst. Wash. Yearbook,* **63,** 152–156.

BROWN, J. D. (1965) A computer program for electron probe analyses. *U. S. Bur. Mines, Rep. Invest.* **6648,** 28 p.

CHALLIS, G. A. (1965) The origin of New Zealand ultramafic intrusions. *J. Petrology,* **6,** 322–364.

CLARK, S. P., AND A. E RINGWOOD (1964) Density distribution and constitution of the mantle. *Rev. Geophys.* **2,** 35–88.

DAVIS, B. T. C., AND F. R. BOYD (1966) The join $Mg_2Si_2O_6$–$CaMgSi_2O_6$ at 30 kilobars and its application to pyroxenes from kimberlites. *J. Geophys. Res.* **71,** 3567–3576.

GREEN, D. H. (1964) The petrogenesis of the high-temperature peridotite intrusion in the Lizard area, Cornwall. *J. Petrology,* **5,** 134–188.

———, AND A. E. RINGWOOD (1967) The stability fields of aluminous pyroxene peridotite and garnet-peridotite and

their relevance in upper mantle structure. *Earth Planet. Sci. Lett.* **3,** 151–160.

———, AND ——— (1970) Mineralogy of peridotite compositions under upper mantle conditions. *Phys. Earth Planet. Interiors,* **3,** 359–371.

———, ———, AND A. MAJOR (1966) Friction effects on pressure calibration in a piston-cylinder apparatus at high pressure and temperatures. *J. Geophys. Res.* **71,** 3589–3594.

HIMMELBERG, G. R., AND R. A. LONEY (1973) Petrology of the Volcan Peak Alpine-Type peridotite, Southwest Oregon. *Geol. Soc. Am. Bull.* **84,** 1585–1600.

ITO, K., AND G. C. KENNEDY (1967) Melting and phase relations in a natural peridotite to 40 kilobars. *Amer. J. Sci.* **265,** 519–539.

JOHANNES, W., P. M. BELL, H. K. MAO, A. L. BOETTCHER, D. W. CHIPMAN, J. F. HAYS, R. C. NEWTON, AND F. SEIFERT (1971) An interlaboratory comparison of piston-cylinder pressure calibration using the albite-breakdown reaction. *Contrib. Mineral. Petrology,* **32,** 24–38.

KUSHIRO, I., AND H. S. YODER (1966) Anorthite-forsterite and anorthite-enstatite reactions and their bearing on the basalt-eclogite transformation. *J. Petrology,* **7,** 337–362.

KUTOLIN, V. A., AND V. M. FROLOVA (1970) Petrology of ultrabasic inclusions from basalts of Minusa and Transbachalian Region (Siberia, USSR). *Contrib. Mineral. Petrology,* **29,** 163–179.

LONEY, R. A., G. R. HIMMELBERG, AND R. G. COLEMAN 1971) Structure and petrology of the Alpine type peridotite at Burro Mountain, California, U.S.A. *J. Petrology,* **12,** 245–309.

MACGREGOR, I. D. (1962) *Geology, petrology, and geochemistry of the Mount Albert and associated ultramafic bodies of Central Gaspe, Quebec.* Master of Science Thesis, Queen's University, Kingston, Ontario.

——— (1964) The reaction 4 enstatite + spinel $\rightleftarrows$ forsterite + pyrope. *Carnegie Inst. Wash. Yearbook,* **63,** 157.

——— (1965a) Stability fields of spinel and garnet peridotites in the synthetic system MgO–CaO–Al_2O_3–SiO_2. *Carnegie Inst. Wash. Yearbook,* **64,** 126–134.

——— (1965b) Aluminous diopsides in the three phase assemblage diopside solid solution + forsterite + spinel. *Carnegie Inst. Wash. Yearbook,* **64,** 134–135.

——— (1967) Mineralogy of model mantle composition. In, P. J. Wyllie, Ed. *Ultramafic and Related Rocks.* New York, John Wiley and Sons, 382–393.

——— (1970) The effect of CaO, Cr_2O_3, Fe_2O_3, and Al_2O_3 on the stability of spinel and garnet peridotites. *Phys. Earth Planet. Interiors,* **3,** 372–377.

———, AND A. E. RINGWOOD (1964) The natural system enstatite-pyrope. *Carnegie Inst. Wash. Yearbook,* **63,** 161–163.

MEDARIS, L. G. (1972) High-pressure peridotites in southwestern Oregon. *Geol. Soc. Amer. Bull.* **83,** 41–58.

NIXON, P. H. O., O. VON KNORRING, AND J. M. ROOKE (1963) Kimberlites and associated inclusions of Basutoland; a mineralogical and geochemical study. *Amer. Mineral.* **48,** 1090–1132.

O'HARA, M. J. (1963) The join diopside pyrope at 30 kilobars. *Carnegie Inst. Wash. Yearbook,* **62,** 116–118.

——— (1967a) Mineral facies in ultrabasic rocks. In, P. J. Wyllie, Ed., *Ultramafic and Related Rocks.* New York, John Wiley and Sons, pp. 7–18.

——— (1967b) Mineral paragenesis in ultrabasic rocks. In, P. J. Wyllie, Ed., *Ultramafic and Related Rocks.* New York, John Wiley and Sons, pp. 393–402.

———, AND E. L. P. MERCY (1963) Petrology and petrogenesis of some garnetiferous peridotites. *Trans. Roy. Soc. Edinburgh,* **65,** 251–314.

———, S. W. RICHARDSON, AND G. WILSON (1971) Garnet-peridotite stability and occurrence in crust and mantle. *Contrib. Mineral. Petrology,* **32,** 48–68.

ONUKI, H., AND T. TIBA (1965) Notes on the petrochemistry of ultramafic intrusives—specially, aluminum distribution in co-existing pyroxenes. *J. Jap. Assoc. Mineral. Petrology Econ. Geol.* **53,** 215–227.

OSBORN, E. F., AND A. MUAN (1960) The system MgO–Al_2O_3–SiO_2, plate 3. Phase equilibrium diagrams of oxide systems. *Amer. Ceramic Soc.,* Columbus, Ohio.

RINGWOOD, A. E., I. D. MACGREGOR, AND F. R. BOYD (1964) Petrological constitution of the upper mantle. *Carnegie Inst. Wash. Yearbook,* **63,** 147–152.

ROSS, C. S., M. D. FOSTER, AND A. T. MYERS (1954) Origin of dunites and of olivine-rich inclusions in basaltic rocks. *Amer. Mineral.* **39,** 693–738.

SKINNER, B. J. (1966) Thermal expansion. In, S. P. Clark, Ed., *Handbook of Physical Constants. Geol. Soc. Amer. Mem.* **97,** 75–96.

———, AND F. R. BOYD (1964) Aluminous enstatites. *Carnegie Inst. Washington Year Book* **63,** 163–165.

WHITE, R. W. (1966) Ultramafic inclusions in basaltic rocks from Hawaii. *Contrib. Mineral. Petrology,* **12,** 245–314.

Manuscript received, August 28, 1972;
accepted for publication, June 12, 1973.